Assessment of in-situ bioremediation at a refinery waste-contaminated site and an aviation gasoline contaminated site

Vishvesh K. Bhupathiraju[1], Paula Krauter[2], Hoi-Ying N. Holman[3], Mark E. Conrad[3], Paul F. Daley[2], Alexis S. Templeton[3,4], James R. Hunt[1], Mark Hernandez[1,5] & Lisa Alvarez-Cohen[1,*]
[1]*Department of Civil and Environmental Engineering, University of California, Berkeley, CA 94720, USA;* [2]*Environmental Restoration Center, Lawrence Livermore National Laboratory, Livermore, CA 94550, USA;* [3]*Earth Sciences Division, Lawrence Berkeley National Laboratory, Berkeley, CA 94720, USA;* [4]*Present address: Department of Geological and Environmental Sciences, Stanford University, Stanford, CA 94305, USA;* [5]*Present address: Department of Civil, Environmental and Architectural Engineering, University of Colorado, Boulder, CO 80309, USA (*author for correspondence: e-mail: alvarez@ce.berkeley.edu)*

Abstract

A combination of geochemical, microbiological and isotopic methods were used to evaluate in-situ bioremediation of petroleum hydrocarbons at one site contaminated with refinery waste and a second site contaminated with aviation gasoline at Alameda Point, California. At each site, geochemical and microbiological characteristics from four locations in the contaminated zone were compared to those from two uncontaminated background locations. At both sites, the geochemical indicators of in-situ biodegradation included depleted soil gas and groundwater oxygen, elevated groundwater alkalinity, and elevated soil gas carbon dioxide and methane in the contaminated zone relative to the background. Radiocarbon content of methane and carbon dioxide measured in soil gas at both sites indicated that they were derived from hydrocarbon contaminant degradation. Direct microscopy of soil core samples using cell wall stains and activity stains, revealed elevated microbial numbers and enhanced microbial activities in contaminated areas relative to background areas, corroborating geochemical findings. While microbial plate counts and microcosm studies using soil core samples provided laboratory evidence for the presence of some microbial activity and contaminant degradation abilities, they did not correlate well with either contaminant location, geochemical, isotopic, or direct microscopy data.

Introduction

Petroleum hydrocarbon release from leaking underground storage tanks is a widespread cause of soil and groundwater contamination (U.S. National Research Council 1993). A wide variety of physical, chemical, and biological methods are being considered for restoring contaminated sites (U.S. National Research Council 1994). Because of the potential for effective remediation of subsurface contaminants with minimal intervention and associated low expense, natural attenuation remains an attractive treatment option. Natural attenuation of subsurface hydrocarbon contamination can occur through a variety of processes including in-situ biodegradation by indigenous microorganisms, advection, dilution, dispersion, sorption, and volatilization (McCallister & Chiang 1994; Rifai et al. 1995). Of these processes, biodegradation is the only one that leads to hydrocarbon destruction resulting in the reduction of hydrocarbon mass.

Most petroleum-related hydrocarbons are readily biodegraded by aerobic microorganisms (Gibson & Subramanian 1984). In subsurface environments, the activities of aerobic microorganisms can deplete oxygen levels, producing anaerobic conditions. A number

of studies have demonstrated that petroleum hydrocarbons can be biodegraded in the absence of oxygen with alternate electron acceptors such as nitrate, manganese (IV), iron (III), sulfate and carbon dioxide (e.g. Holliger & Zehnder 1996; Krumholz et al. 1996; Zengler et al., 1999; So & Young, 1999; Ehrenreich et al., 2000), but at rates substantially lower than degradation under aerobic conditions.

Although in-situ bioremediation can be an effective method for treating fuel and other hydrocarbon contamination in soil and groundwater (U.S. National Research Council 1994; Rice et al. 1995), in order for it to be an acceptable remediation option, multiple independent lines of evidence that prove that microorganisms are responsible for contaminant degradation are needed. Potential evidence for in-situ biodegradation is often gathered by comparing geochemical and microbial characteristics in the contaminated zone to those of uncontaminated background areas. Some types of evidence for in- situ biodegradation includes the following observations: (i) decreasing contaminant concentration over time, (ii) consumption of electron acceptors and production of their reduced byproducts, (iii) production of signature degradation intermediates and products, (iv) stable isotopic ratios and radioisotopic content of contaminants and degradation products, and (v) distinct patterns of elevated biomass concentrations and activities. While these observations can provide valuable information supportive of in-situ biological activities, each has inherent interpretational limitations, and, when used alone, can yield ambigious results (U.S. National Research Council 1993; Gieg et al. 1999; Conrad et al. 1999a; Chapelle et al. 1996; Madsen et al. 1991; Hunkeler et al. 1999). However, when used in combination, these observations can provide convincing evidence for the occurrence of in-situ bioremediation (Wiedemeier et al. 1995; Gieg et al. 1999; Cho et al. 1997; Bolliger et al. 1999; Kampbell et al. 1996; Conrad et al. 1999a, b; Hohener et al. 1998; Hunkeler et al. 1999).

In this study, a suite of techniques were applied to evaluate in-situ bioremediation at two petroleum hydrocarbon contaminated sites in Alameda Point, CA. These techniques included: (1) physical and chemical analyses on soil and groundwater samples for evaluation of contaminant loss and degradation mechanisms; (2) microbial enrichment techniques and microcosm assays to provide laboratory confirmation of contaminant degradation; (3) non-culture-based direct epifluorescent microscopy methods to enumerate total and active microbial populations; and (4) isotopic measurements of CO_2, CH_4 and hydrocarbon contaminants to differentiate biodegradation of natural organic matter from biodegradation of hydrocarbon contaminants, and to provide field confirmation of contaminant loss and microbial activity.

Materials and methods

Site background and description

The study sites (Site 13 and Site 3) are located at Alameda Point (formerly Alameda Naval Air Station), on the western end of Alameda Island in the San Fransisco Bay. The hydrogeology and summaries of investigations performed at the study sites are detailed elsewhere (Alvarez-Cohen et al. 1998).

Site 13 covers approximately 30 acres and is located in the southeast corner of Alameda Point. This site is the former location of the Pacific Coast Oil Works refinery, which operated between 1879 and 1903. Refinery wastes were disposed at the site during the 24-year history of the refinery. This site is currently covered with discontinuous asphalt and weeds. The distribution of total petroleum hydrocarbons (TPH) found between 1.5 to 3.0 m depth below ground surface (bgs) in 1994 at Site 13 is shown in Figure 1. There is no significant horizontal groundwater movement at this site (Alvarez-Cohen et al. 1998), but the water table fluctuates between 0.9 and 1.6 m depth.

Site 3 is a two acre, abandoned fuel storage area, where approximately 365,000 gallons of aviation gasoline (AVGAS) is estimated to have leaked from storage tanks in the 1960s and early 1970s. Currently, the central and the northeastern part of Site 3 is covered by irrigated grass, and the rest of the area is covered by asphalt roadways and a parking lot (Figure 2). The central grassy area was the area originally impacted by the AVGAS release. Hydrocarbon materials including TPH, gasoline range organic compounds (GROs), and AVGAS were detected in soil, soil gas and groundwater samples from several locations at Site 3 (Conrad et al. 1999a; Alvarez-Cohen et al. 1998; PRC Environmental Management & Montgomery Watson 1993). The distribution of gasoline range organic compounds (GROs) in soil gas samples measured during 1996 at site 3 are shown in Figure 2. The water table at this site fluctuates between depths of 1.0 and 1.9 m and the general direction of groundwater flow is believed to be to the northwest.
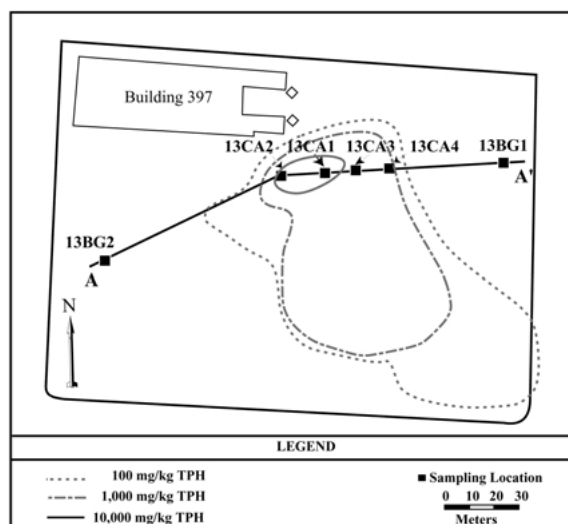
Figure 1. Schematic representation of Site 13 showing the distribution of total petroleum hydrocarbons (TPH) previously measured in soil between 1.5 and 3.0 m depth and the sampling locations for microbial and geochemical analyses.

Figure 2. Schematic representation of Site 3 showing the distribution of gasoline range organic compounds (GROs) in soil gas samples and the sampling locations for microbial and geochemical analyses. Also shown are the former locations of the fuel storage tanks in the central grassy area.

Sampling locations and methods

Samples for microbial and geochemical analyses were collected from six locations at each site (Figures 1 and 2). Four of the sampling locations, designated CA1 thru CA4, were located within the areas of contamination. Two of the sampling locations, designated BG1 and BG2, were located outside of the areas of contamination and were considered background samples. Samples from site 13 were collected between July 30, 1996 and September 5, 1996. Samples from site 3 were collected between November 11, 1996 and December 2, 1996.

Soil core samples were extracted using Geoprobe 5400 Direct Penetration Technology (DPT) equipped with a MacroCore continuous sampling device. The sampling device was steam sterilized in the field prior to each sampling. At each location, soils were sampled at a total depth of 4.9 m (bgs) using sterilized, 4 cm by 120 cm polyethylene terephthalate glycol (PETG) sampling tubes. Upon retrieval of each sample, the sampling tube was removed from the sampling device, capped with sterilized end caps, and stored on ice in a cooler until they were transported to the laboratory for analyses. Upon completion of soil sampling, a small well was bored adjacent to the soil sampling location and groundwater samples were extracted for geochemical analyses. To obtain groundwater samples, an E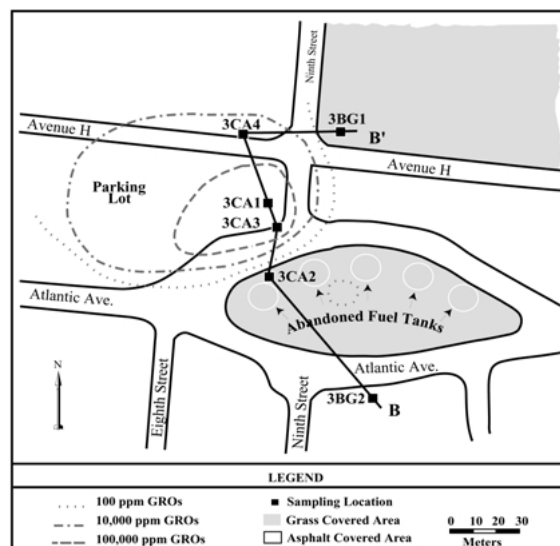nvironment Equipment Model SP-T-15-24 stainless steel bladder pump fitted with teflon components was used to purge each well. For wells that yielded groundwater at sufficient rates, approximately three casing volumes of water was purged prior to sample collection. All groundwater samples were collected directly from the pump discharge line into sample containers, sealed and stored on ice prior to analysis. Analyses were completed within 24 h. Soil gas samples were collected from probes installed throughout the site and in the immediate vicinity of the soil and groundwater sampling locations. The sampling probes consisted of hollow 1/4 inch outer diameter (O.D.) stainless steel tubes installed to the depth of sampling and fitted at the surface with 3/8 inch O.D. tygon tubing for sample collection. Soil gas samples were collected in Tedlar bags using a peristaltic pump. Prior to sampling, a minimum of three volumes of gas was purged from each probe. Approximately 1 to 1.5 L of gas was collected in Tedlar bags at a flow rate of 50 to 100 cc/minute.

Geochemical analyses

Unless otherwise noted, geochemical analyses of groundwater samples were performed in the field. Conductivity measurements at both sites were performed using a Beckman 11 monitoring system (Alvarez-Cohen et al. 1998). Dissolved oxygen, fer-

rous iron, ammonium, and sulfide in groundwater were measured using Hach test kits (Hach Company, Loveland, CO). Nitrate and nitrite in the groundwater from Site 13 were measured using CHEMetrics test kits (CHEMetrics, Calverton, VA). The total alkalinity in groundwater from Site 13 was measured using a Hach test kit (Hach Company, Loveland, CO). Analyses of nitrate, nitrite, iron, manganese, sulfate, total alkalinity, chloride, potassium, calcium, sodium, and magnesium in the groundwater from Site 3 was performed within 24 h of sampling by a commercial laboratory using standard EPA methods (California Laboratory Services, Livermore, CA). Carbon dioxide, oxygen, and methane in soil gas samples were analyzed by gas chromatography (Chu & Alvarez-Cohen 1998). Radiocarbon (^{14}C) in soil gas was measured using the accelerator mass spectrometer (AMS) at Lawerence Livermore National Laboratory, and reported as a fraction of modern carbon. Sample preparation was as previously described (Conrad et al. 1999a, b).

Soil microbial analyses

Microbial biomass and activity in soil cores collected from each site were examined using direct epifluorescent microscopy, microbial enrichments, and microcosms. Soil core samples collected for these analyses were processed within 12 to 24 h of collection. For Site 13, soil cores from 0.4, 0.9, 1.6, 2.3, and 3.1 m depth were analyzed. For Site 3, soil cores from 0.5, 1.0, 1.9, 2.3, and 3.4 m depth were analyzed.

Total bacterial biomass and active bacterial biomass in soils were determined by a direct microscopy method employing the activity stain, 5-cyano-2,3-ditolyl tetrazolium chloride (CTC), and the cell wall stain, 5-(4,6-dichlorotriazinyl) aminofluorescein hydrochloride (DTAF) (Bhupathiraju et al. 1999a, b). Twenty-five grams of soil from each core were mixed with sterile phosphate buffer (pH 7.2) containing 0.1% sodium pyrophosphate and diluted to 250 mL final volume. Soil suspensions were mixed on a shaker at 160 rpm for approximately four hours in order to break up soil clumps. A series of dilutions were then made from each soil suspension and incubated for four hours in tubes containing CTC staining solution prior to counter-staining with DTAF. This method has been shown to be effective for counting both aerobic and anaerobic cells (Bhupathiraju et al. 1999b). The stained aliquots were filtered onto black polycarbonate membrane filters and examined by direct epifluorescent microscopy. Cells that retained the green fluorescence from DTAF were counted as the total biomass while cells that retained DTAF fluorescence together with bright intracellular orange CTC-formazan deposits were identified as active bacteria. A minimum of ten random microscopic fields were counted and averaged. Microbial biomass was normalized to the dry weight of total suspended solids (TSS) of the soil dilutions; TSS was determined according to standard methods (APHA 1995).

Culturable heterotrophic bacteria and actinomycetes in soil were enumerated aerobically using standard heterotrophic plate count (HPC) and actinomycete plate count (APC) techniques. Ten grams of soil were diluted in a 100 ml solution containing 0.1% sodium pyrophosphate and mixed on a shaker at 160 rpm for 15 minutes. Aqueous suspensions of the soil slurries were serially diluted in 0.1% sodium pyrophosphate solution. Aliquots were plated in triplicate on PTYG media (Ghiorse & Balkwill 1983) and actinomycete culture media (Atlas 1993) to enumerate HPCs and APCs, respectively. Individual colonies were counted after a 28 day incubation period at room temperature. Fungi were enumerated by distributing undiluted soil (0.5-1.0 g) evenly on the surface of Sabourauds Dextrose agar-Emmons agar plates (Sinclair & Ghiorse 1989). Fungal colonies or outgrowths from the distributed soil particles were counted after 7 and 14 days of incubation at room temperature. Sulfate-reducing and iron-reducing bacteria were enumerated using a commercially available assay kit (BART[TM] Droycon Bioconcepts Inc., Regina, Canada), following the manufacturer's instructions.

Microcosm studies were conducted under static, aerobic conditions with unsaturated soil samples (Holman & Tsang 1995). Microcosms consisted of a 30 mL glass extraction thimble placed on top of a supporting ring inside a 250 mL gas-tight mason jar. A small tube containing 2N NaOH was suspended in the mason jar to trap CO_2. A dilute H_2O_2 solution was used to maintain aerobic conditions ($O_2 \geq 19\%$) inside the mason jar. Experiments were initiated by loading 36 grams of soil into the thimble and adding ^{14}C-labeled hydrocarbon solutions (ring-^{14}C-p-xylene [50 ppb] for site 13 microcosms and n-hexadecane-1-[14]C [2000 ppm] for Site 3 microcosms). The labeled hydrocarbon was chosen to represent a specific target contaminant observed at each site. The concentration of the labeled hydrocarbons was chosen based on concentrations measured in field samples. Two viable and one sterilized microcosm (4-overnight freeze/thaw

cycles followed by azide treatment) were prepared for each soil sample to serve as controls. To monitor the production of $^{14}CO_2$ from ^{14}C-labeled hydrocarbons, samples were retrieved from the NaOH trap every 3.5 days, and transferred to scintillation fluid for quantification using a liquid scintillation counter. The $^{14}CO_2$ production in the microcosms was monitored over a 45-day period.

Results

Site 13

The geochemical characteristics of groundwater and soil gas collected from Site 13 are listed in Table 1. Patterns consistent with microbiological activity were observed. Groundwater dissolved oxygen content varied with respect to contamination levels. The dissolved oxygen levels in groundwater from the background sample locations (13BG1 and 13BG2) were high (4.3 and 4.9 mg/L, respectively), while the groundwater from sample locations 13CA1 and 13CA2 in the high contamination area contained no detectable dissolved oxygen. The groundwater from the low concentration contaminant area (13CA3 and 13CA4) contained dissolved oxygen at levels slightly lower (3.0 to 4.0 mg/L) than the background. The levels of nitrate and nitrite in groundwater from all sample locations at Site 13 were very low (<1 mg/L), with the exception of location 13CA3 that contained some nitrate (2.9 mg/L). Some ammonium was detected in groundwater from all sample locations, with the highest values occurring in the high contamination locations 13CA2 and 13CA1. Ferrous iron and sulfide concentrations in the groundwater were very low (<0.7 mg/L).

Although groundwater sulfate levels were not analyzed at this site, sulfate was detected in soil samples. Soil sulfate levels near the water table depth (0.9 to 1.6 m) in the contaminated areas ranged from 25 to 180 mg/kg, while those in the background areas ranged from 20 to 55 mg/kg. The total alkalinity in the groundwater from sample locations 13CA1 and 13CA2 in the high contamination area was substantially higher (540 and 550 mg/L, respectively) than that observed in groundwater from either the background areas or the areas containing lower contamination levels. Little variation was observed in conductivity measurements of the groundwater from the contaminated areas relative to the background, suggesting little seawater influence at this site.

The content and isotopic composition of soil gas at this site exhibited significant seasonal fluctuation, with high methane production occurring predominantly in May to July, after the spring rains had ceased (Conrad et al. 1999b). Soil gas data collected during the period of highest methane accumulation, June and July of 1996, are shown in Table 1. Soil gas from 13CA1 and 13CA2 in the high contamination area, contained high levels of CH_4 (up to 63% v/v), elevated CO_2 levels (up to 13% v/v), and depleted O_2 levels (as low as 0% v/v). The ^{14}C content of the soil gas CH_4 and CO_2 from this area was relatively low (0.03 and 0.28–0.30 times modern carbon, respectively) suggesting hydrocarbon origin. In contrast, soil gas samples from the low contamination area (13CA3 and 13CA4) and background areas (13BG1 and 13BG2) contained near atmospheric levels of O_2 (19.4–21.8 % v/v), trace levels of CO_2 (0.1–1.5 % v/v), and no detectable CH_4. The ^{14}C content of the soil gas CO_2 from the low contamination areas and background areas was relatively high (0.63 and 0.66 times modern carbon, respectively), suggesting non-hydrocarbon origin. Cellular staining and direct microscopy indicated the presence of high numbers of bacteria in all of the soils examined at Site 13 (Figure 3). Soils from sample locations 13CA2 and 13CA3 in the high and low contamination areas, respectively, contained the highest amounts of bacterial biomass (ranging from 9×10^8 to 6.2×10^9 cells/g soil; Figure 3A) and active bacteria (ranging from 4×10^8 to 2.8×10^9 cells/g soil; Figure 3B). The total and active bacterial biomass in soils from 13CA1 and 13CA4 were slightly lower. In all cases, the highest numbers of total and active bacteria were detected at or below the water table. The background locations exhibited total and active biomass numbers that were approximately an order of magnitude lower than those detected in the soils from the contaminated locations.

Culturable aerobic microorganisms were present in most of the soils from Site 13. The HPCs were higher in soils from shallow depths, and counts declined with increasing depth across the entire site (Figure 4A). In general, soils from sample locations 13CA2, 13CA3 and 13CA1 in the contaminated areas and soils from sample location 13BG1 in the background area yielded the highest HPC numbers (Figure 4A). A similar trend was observed with APC numbers (data not shown). Soil samples from Site 13 also contained significant, but lower populations of culturable fungi, with background location numbers ranging from 34 to 593 propagules/g dry soil, and contaminated location numbers ranging from 17 to 1000 propagules/g

Table 1. Groundwater and soil gas parameters from Site 13 sampling locations

Parameter	Sampling location					
	13BG2	13CA2	13CA1	13CA3	13CA4	13BG1
Groundwater						
Dissolved oxygen (mg/L)	4.9	<0.1	<0.1	4.0	3.0	4.3
Nitrate (mg/L)	0.9	<0.4	<0.4	2.9	<0.4	0.8
Nitrite (mg/L)	<0.1	<0.1	<0.1	6.5	<0.1	7.3
Ammonium (mg/L)	0.3	0.9	2.8	0.8	0.5	0.3
Ferrous iron (mg/L)	0.2	<0.1	0.5	0.1	<0.1	0.1
Sulfide (mg/L)	0.3	0.1	0.5	0.6	0.2	0.7
Total alkalinity as $CaCO_3$ (mg/L)	250	550	540	220	180	290
Conductivity (μS)	538	770	1050	810	340	870
Soil gas						
Sampling depth (m)	1.20	0.45	0.60	0.45	0.45	0.60
Oxygen (%)	21.8	2.5	0.0	21.7	21.8	19.4
Carbon dioxide (%)	0.0	13.0	2.7	0.1	0.0	1.5
Methane (%)	0.0	10.3	62.5	0.0	0.0	0.0
^{14}C content of carbon dioxide (times modern)	–	0.28	0.30	0.63	–	0.66
^{14}C content of methane (times modern)	–	nd	0.03	–	–	–

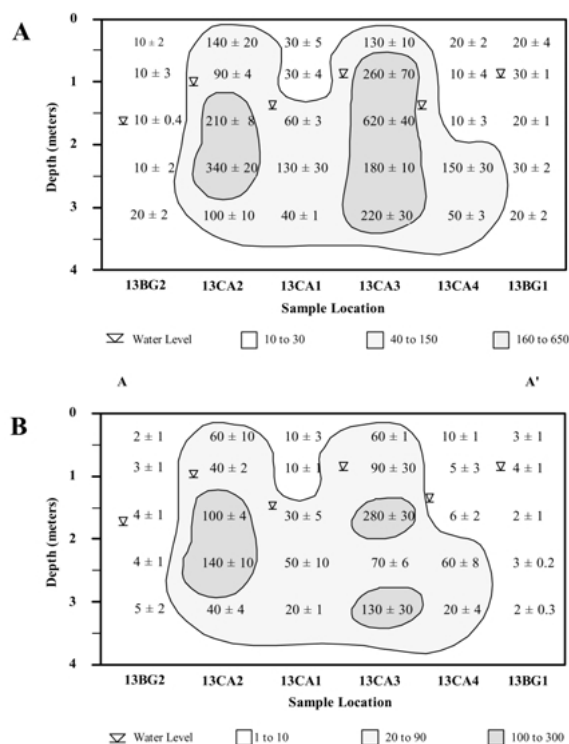[a] nd, not determined; –, not applicable.

Figure 3. Total (A) and Active (B) bacteria ($\times 10^7$ cells/gram) in Site 13 soils. Data are averages of triplicates $\pm$ standard deviation.

dry soil. Culturable sulfate-reducing bacteria and iron-reducing bacteria were observed in soils obtained from 1.6 and 2.3 m depth from background location 13BG2 (below detection and 10^6 cfu/g dry soil, respectively) and contaminated location 13CA2 ($\geq 10^6$ cfu/g dry soil for both).

Microcosm studies were conducted to test the ability of the microbial populations in site 13 soils to aerobically mineralize p-xylene. Less than 5% [^{14}C] p-Xylene mineralization was observed for all samples (Figure 4B). The mineralization period for most of the locations lasted throughout the 45-day incubation period. Observed biodegradation lag phases were less than six days and were similar in replicates from all locations. Although there was no observable statistical trend with respect to mineralization activity and contaminant location or depth, samples retrieved from high contaminant locations 13CA2 and 13CA1, low contaminant location 13CA3, and background location 13BG1 were highest at the 1.6 m depth, just below the water table, and decreased with vertical distances away from the water table.

Site 3

The geochemical characteristics of groundwater and soil gas collected from Site 3 are summarized in Table 2. Two sample locations at Site 3 were in grass covered
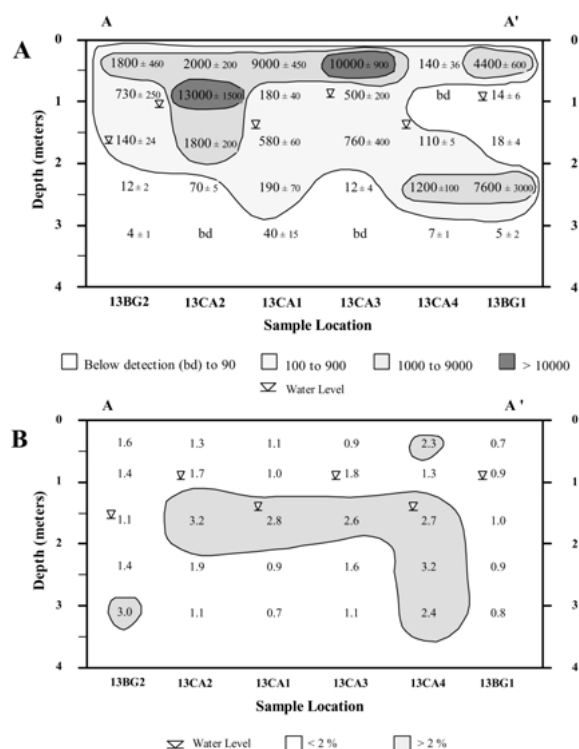
Figure 4. (A) Heterotrophic bacterial plate counts ($\times 10^2$ CFU/gram) in Site 13 soils. Data are averages of triplicates $\pm$ standard deviation. (B) The percent of $^{14}CO_2$ produced from [^{14}C] p-Xylene mineralization in Site 13 soil microcosms. Date are averages of duplicates and corrected for radioactivity recovered as $^{14}CO_2$ in controls.

areas, a background location (3BG1) and a low contamination location (3CA2), while the remaining four sample locations were asphalt covered (Figure 2). The groundwater dissolved oxygen was highest in the two grass covered locations (1.0 mg/L and 2.4 mg/L at 3BG1 and 3CA2, respectively), while two of the asphalt covered locations in the contamination zone (3CA1 and 3CA4) contained no detectable dissolved oxygen and the asphalt covered background (3BG2) and high contamination zone (3CA3) location had very low dissolved oxygen (0.7 mg/L). In addition, soil gas samples indicated significantly depleted oxygen concentrations in all asphalt covered contaminated locations (Table 2).

The nitrate and nitrite levels in the groundwater from Site 3 were low. Ammonium was consistently detected in groundwater from all sample locations, with the highest concentrations found at the two asphalt covered high contamination locations (3CA3 and 3CA1) and the grass covered background location 3BG1. Ferrous iron, manganese, and sulfide

in groundwater were not correlated with asphalt or grass cover, with high or low contamination zones, or with background locations. Extremely high manganese (390 mg/L) was measured at one high contamination asphalt covered location (3CA3). Sulfate concentrations in groundwater from both the asphalt covered background location 3BG2 and the grass covered background location 3BG1 were high (210 and 290 mg/L, respectively). The sulfate levels in groundwater from the contaminated sample locations were substantially lower than the background locations (5 to 14 mg/L) with the exception of the asphalt covered 3CA3 sample location (210 mg/L). Alkalinity values were elevated throughout the site. The conductivity measurements, and the concentrations of calcium, chloride, magnesium, phosphate and sodium in the groundwater from the high contamination locations 3CA3, 3CA1, and the grassy background 3BG1 were significantly higher than those observed in other sampling locations (Table 2, Table 3), suggesting the presence of some seawater influence in portions of this site.

The composition of soil gas across this site did not exhibit significant seasonal fluctuation (Conrad et al. 1999a). Soil gas from the asphalt covered sampling locations 3CA1 and 3CA3 in the high contamination area contained high levels of both CH_4 (22.3–24.7 % v/v) and CO_2 (12.4–18.3% v/v), and depleted levels of O_2 (1.2–1.4% v/v) (Table 2). Soil gas from the asphalt covered, low contamination location 3CA4, was low in CH_4 (1.6 % v/v) and O_2 (1.8% v/v), but relatively high in CO_2 (10% v/v). On the other hand, soil gas from the grass covered contaminant location 3CA2 contained high levels of O_2 (12.3 % v/v) and CO_2 (7.1% v/v) but had no detectable CH_4. The ^{14}C content of the soil gas CH_4 and CO_2 from the asphalt covered contaminated areas was extremely low (<0.1 times modern carbon), suggesting hydrocarbon origin. In contrast, soil gas samples from the background locations (3BG1 and 3BG2) contained near atmospheric levels of O_2 (20.4–21.0% v/v), trace levels of CO_2 (0.7–1.7% v/v), and no detectable CH_4. The ^{14}C contents of the soil gas CO_2 from the grass covered low contamination location 3CA2 and background location 3BG1 were significantly higher (0.61 and 0.90 times modern carbon, respectively), suggesting atmospheric or natural organic matter origin.

The direct microscopy estimates of microbial biomass in soils sampled at Site 3 are shown in Figure 5. Soils from the grass-covered and asphalt-covered low contaminant location 3CA2 and 3CA4, and the

Table 2. Groundwater and soil gas parameters from Site 3 sampling locations

Parameter	Sampling location					
	3BG2	3CA2	3CA3	3CA1	3CA4	3BG1
Groundwater						
Dissolved oxygen (mg/L)	0.7	2.4	0.7	<0.1	<0.1	1.0
Nitrate (mg/L)	2.3	<0.5	<50	2.9	0.6	<0.5
Nitrite (mg/L)	<0.5	<0.5	<50	<0.5	<0.5	<0.5
Ammonium (mg/L)	4.3	2.7	15.9	10.0	1.7	10.7
Ferrous iron (mg/L)	0.3	0.8	3.8	0.9	4.7	2.6
Manganese (mg/L)	0.4	<0.03	390	0.6	1.1	1.3
Sulfide (mg/L)	0.01	0.54	0.23	0.04	0.42	0.33
Sulfate (mg/L)	210	14	210	12	5	290
Alkalinity as $CaCO_3$ (mg/L)	1200	600	3800	1800	580	1500
Conductivity (μS)	550	780	22000	10200	1510	9200
Chloride (mg/L)	1400	45	9300	2700	200	2200
Potassium (mg/L)	50	21	200	85	41	74
Soil gas						
Sampling depth (m)	1.20	0.90	1.20	1.20	0.60	0.60
Oxygen (%)	21.0	12.3	1.2	1.4	1.8	20.4
Carbon dioxide (%)	0.7	7.1	12.4	18.3	10.4	1.7
Methane (%)	0.0	0.0	22.3	24.7	1.6	0.0
^{14}C content of carbon dioxide (times modern)	nd	0.61	nd	0.05	nd	0.90
^{14}C content of methane (times modern)	–	–	0.07	0.05	nd	–

[a] nd, not determined; –, not applicable.

asphalt-covered high contaminant location 3CA3 contained the highest amount of total bacterial biomass (4 $\times$ 10^8 to 2.5 $\times$ 10^9 cells/g soil) and active bacteria (2 $\times$ 10^8 to 1.6 $\times$ 10^9 cells/g soil). The total and active bacterial biomass in soils from the asphalt covered high contaminant location 3CA1 was slightly lower, and those from the background locations were significantly lower than those detected in the contaminated soils.

Detectable numbers of culturable aerobic microorganisms were found in most of the soils from Site 3 (Figure 6A). In general, HPCs were higher in soils from shallow depths, and declined with increasing depth. Shallow soils from the grass covered low contamination location 3CA2, asphalt-covered high contamination location 3CA1, and the background location 3BG2 yielded the highest HPC numbers (Figure 6A) and APCs (data not shown). Culturable fungi were also observed in soil samples examined at Site 3, but did not follow any discernable pattern, with background location numbers ranging from 14 to 280 propagules/g dry soil and contaminated location numbers ranging from 6 to 1300 propagules/g dry soil. Iron-reducing bacteria and sulfate-reducing bacteria

were enumerated in soils obtained from 1.0, 1.9, and 2.3 m depths at asphalt covered locations 3BG2, and 3CA1, 3CA3 and 3CA2. Iron-reducing bacteria were higher in the background (10^4 to 10^6 cfu/g dry soil) than in the contaminated locations (below detection for 3CA4, 10^4 CFU/g dry soil for 3CA1 and 3CA3). Sulfate-reducing bacteria were present in the background location at numbers similar to those at 3CA3 in the contaminated area (10^5 to 10^6 cfu/g dry soil), but were below detection at 3CA1 and 3CA4.

Microcosm studies were conducted to test the ability of the site 3 soil communities to aerobically mineralize n-hexadecane. The $^{14}CO_2$ produced from n-Hexadecane-1-^{14}C is shown in Figure 6B. The mineralization period for all locations lasted throughout the 45-day incubation period. At the background locations, 3BG1 and 3BG2, the mineralization activities were relatively high for almost all depth intervals, while those from the contaminated locations varied over depth and location.
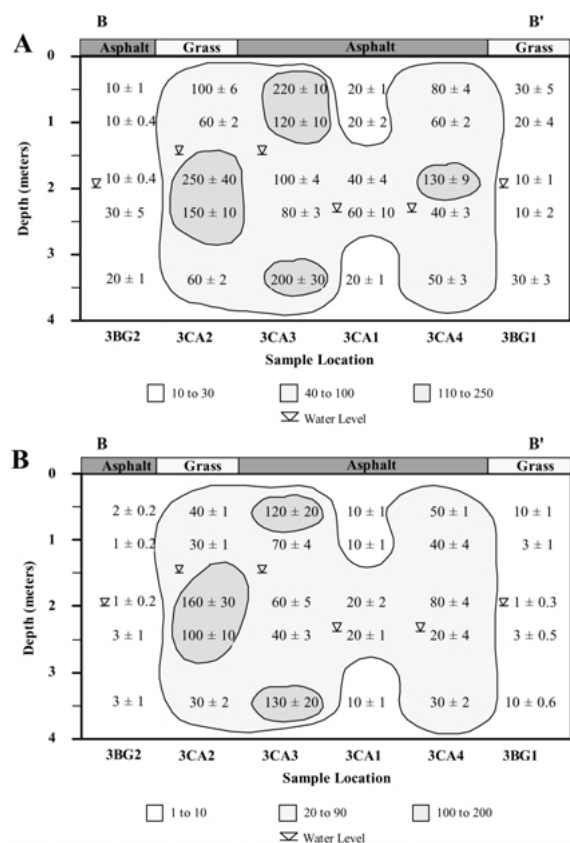
Figure 5. Total (A) and Active (B) bacteria ($\times 10^7$ cells/gram) in Site 3 soils. Data are averages of triplicates $\pm$ standard deviation.

Figure 6. (A) Heterotrophic bacterial plate counts ($\times 10^2$ CFU/gram) in Site 3 soils. Data are averages of triplicates $\pm$ standard deviation. (B) The percent of $^{14}CO_2$ produced from [^{14}C] n-Hexadecane mineralization in Site 3 soil microcosms. Data are averages of duplicates and corrected for radioactivity recovered as $^{14}CO_2$ in controls.

Discussion

At both study sites described in this manuscript, multiple lines of evidence based upon geochemistry, non-culture based microscopy, and isotopic measurements suggested that in-situ biodegradation was resulting in contaminant destruction. At Site 13, the depleted oxygen and elevated alkalinity in groundwater from the contaminated locations compared to groundwater from the background locations suggest significant biodegradation activity in the high contamination zone, and lower levels of activity in the low contamination locations. Radiocarbon contents of the soil gases from the high contamination locations indicated that approximately 70% of the CO_2 is a product of hydrocarbon degradation in the high contamination zone, while only around one third is from hydrocarbons in the low contamination locations (Table 1; Conrad et al. 1999b).

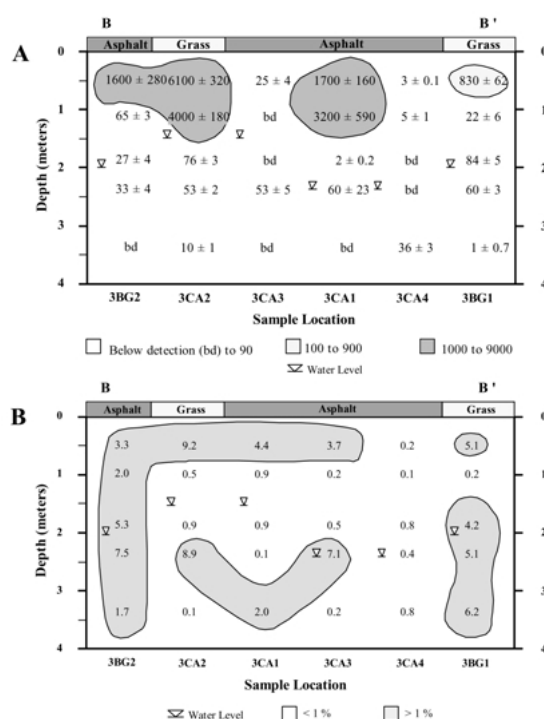The low levels of potential alternate electron acceptors, such as nitrate, and reduced respiration products, such as nitrite and ferrous iron in groundwater from both background and contaminated locations suggest that nitrate reduction and iron reduction may not be important mechanisms of hydrocarbon degradation at Site 13. It is unclear whether sulfate reduction is an important process at this site. While sulfate-reducing bacteria and sulfate were detected in soils from Site 13, no discernable pattern indicative of sulfate consumption was apparent in the contaminated zone. Also, the levels of sulfide in groundwater from the contaminated areas did not differ significantly from the background areas (Table 1). Of course, it is possible that precipitation affected concentrations of both sulfide and ferrous iron at this site. Conductivity measurements indicated that the groundwater from Site 13 is not significantly influenced by seawater (Table 1), a potential source of sulfate. Even if some sulfate reduction was occurring at Site 13, the lack of sulfate input at the site suggests that sulfate-dependent anaerobic hydrocarbon degradation would not be sustainable.

The presence of significant quantities of methane in soil gas from the contaminated areas suggests that anaerobic and methanogenic degradation processes are occurring at Site 13. The levels of methane detected in the soil gas (Table 1) suggest that the methanogenic activity is confined to the high contamination areas (13CA1 and 13CA2). The radiocarbon content of the soil gas methane from these areas was extremely low (<0.1 times modern), suggesting that the methane was derived from subsurface contaminant degradation. Stable carbon isotope measurements of soil gas CO_2 and CH_4 at this site suggested that methanogenesis predominantly occurs at or near the water table surface, possibly acting on hydrocarbons that have previously undergone partial oxidation (Conrad et al. 1999b). Stable isotopic evidence suggests that as the methane diffuses up towards the ground surface, it becomes oxidized by methanotrophic organisms (Conrad et al. 1999b).

At Site 3, the depleted oxygen levels in groundwater and soil gas (Table 2) from the contaminated zone and the elevated soil gas CO_2 and CH_4 suggest high biodegradation activity currently occurs in the asphalt covered locations and lower degradation activity in the grass covered location. Radiocarbon analysis (Table 2) of the soil gases indicate that the CO_2 and CH_4 produced in the asphalt covered locations were predominantly products of hydrocarbon degradation. These data are consistent with the hypothesis that aerobic contaminant degradation previously occurred in the grass covered contamination zone resulting in rapid depletion of hydrocarbons while hindered oxygen transport in the asphalt covered areas resulted in slower hydrocarbon remediation.

The low levels of nitrate and iron (II) in groundwater from both background locations and contaminated zones suggest that iron reduction and nitrate reduction may not be important mechanisms of hydrocarbon degradation at Site 3, however manganese oxidation may be occurring. The groundwater from some of the sampling locations at Site 3 had high conductivity and dissolved ion concentrations indicative of seawater infiltration (Table 2), suggesting that sulfate may be available as a terminal electron acceptor for the oxidation of petroleum hydrocarbons under anaerobic conditions. Significant sulfate depletion was not apparent in either of the background locations or in the grass-covered contaminant location (3CA2). Since seawater intrusion could provide a constant supply of sulfate to the asphalt-covered subsurface, sulfate-associated hydrocarbon oxidation may represent a major mech-

anism for natural attenuation of contaminants in this portion of Site 3. High levels of methane in the high contamination zone indicate that methanogenic degradation is also occurring underneath the asphalt at Site 3.

At both Site 13 and Site 3, field evidence gathered from groundwater, soil gas and isotope monitoring techniques clearly suggest the presence of biodegradation activity in the contaminated zones. Consistent with these lines of evidence, direct microscopy results indicated the presence of increased microbial numbers and activity within the contaminated zones compared to background locations (Figures 3 and 4). In contrast, data from microbial plate counts and microcosm experiments did not correlate well with geochemical data or with levels of subsurface contamination, providing inconclusive evidence of microbial activities in the soils. In general, the microbial enumerations obtained from plate count assays were several orders of magnitude lower than those obtained with direct microscopy. This is not unexpected since plate counts will not detect slow-growing and non-culturable microorganisms, and cells that require specific redox and nutrient conditions not provided by the chosen culture conditions. Since groundwater geochemical parameters clearly suggest that anaerobic conditions exist in the contamination zones at both Site 13 and Site 3, and since the direct microscopy technique used in this study is capable of detecting both aerobic and anaerobic microorganisms (Bhupathiraju et al. 1999b), it is reasonable to assume that part of the discrepancy between the plate counts and the direct microscopy results were due to substantial anaerobic microbial population present in the subsurface at Site 13 and 3. However, culture-based analysis techniques to quantify anaerobic iron-reducing and sulfate-reducing bacteria also yielded substantially low and inconsistent results, possibly due to the inherent limitations of conventional culture-based techniques. The contaminant degradation activity that was apparent from the field data was also not realized in the laboratory microcosm experiments, which showed low and/or inconsistent biodegradation potential in the soils (measured as mineralization). Although the inconsistent biodegradation potential observed in microcosms may be partially attributed to the choice of added substrate, the microcosm design, and the predominance of anaerobic activity in some locations at the sites, there was no consistent pattern with site contamination levels or geochemical data. In this study, non-culture-based direct microscopy approaches with redox stains that

quantitate aerobic and anaerobic microbial populations were more effective than culture-based methods such as plate counts and microcosms to gauge microbial activity associated with in-situ bioremediation.

Acknowledgements

References

Alvarez-Cohen L, Bhupathiraju VK, Conrad ME, Daley PF, Holman HN, Hunt JR, Krauter P, McDonald M & Udell K (1998) Intrinsic Bioremediation, Sites 13 and 3, Alameda Point, California; Treatability Study Report. Contract No. N62474-94-D-7430; Delivery Order No. 005; Submitted to Department of Navy, Engineering Field Activity, West, Naval Facilities Engineering Command, San Bruno, California

APHA (1995) Standard methods for the examination of water and wastewater. In: Eaton AD, Clesceri LS & Greenberg A (Eds). American Public Health Association, Washington, DC

Atlas RM (1993) Handbook of Microbiological Media. Parks LC (Ed). CRC Press, Ann Arbor, Michigan

Bhupathiraju VK, Hernandez M, Krauter P & Alvarez-Cohen L (1999a) A new direct microscopy based method for evaluating in-situ bioremediation. J. Hazard. Mater. B67: 299–312

Bhupathiraju VK, Hernandez M, Landfear D & Alvarez-Cohen L (1999b) Application of a tetrazolium dye as an indicator of viability in anaerobic bacteria. J. Microbiol. Meth. 37: 231–243

Bolliger C, Hohener P, Hunkeler D, Haberli K & Zeyer, J (1999) Intrinsic bioremediation of a petroleum hydrocarbon-contaminated aquifer and assessment of mineralization based on stable carbon isotopes. Biodegradation 10: 201–217

Chapelle FH, Bradley PM, Lovley DR & Vroblesky DA (1996) Measuring rates of biodegradation in a contaminated aquifer using field and laboratory methods. Ground Water 34: 691–698

Cho JS, Wilson JT, DiGiulio DC, Vardy JA & Choi Q (1997) Implementation of natural attenuation at a JP-4 jet fuel release after active remediation. Biodegradation 8: 265–273

Chu KH & Alvarez-Cohen L (1998) Effect of nitrogen source on growth and trichloroethylene degradation by methane-oxidizing bacteria, Appl. Environ. Microbiol. 64: 3451–3457

Conrad ME, Templeton AS, Daley PF & Alvarez-Cohen L (1999a) Isotopic evidence for biological controls on migration of petroleum hydrocarbons. Org. Geochem. 30: 843–859

Conrad ME, Templeton AS, Daley PF & Alvarez-Cohen L (1999b) Seasonally-induced fluctuations in microbial production and consumption of methane during bioremediation of aged subsurface refinery contamination. Environ. Sci. Technol. 33: 4061–4068

Ehrenreich P, Behrends A, Harder J & Widdel F (2000) Anaerobic oxidation of alkanes by newly isolated denitrifying bacteria. Arch. Microbiol. 173(1): 58–64

Ghiorse WC & Balkwill DL (1983) Enumeration and morphological characterization of bacteria indigenous to subsurface environments. Develop. Indust. Microbiol. 24: 213–224

Gibson DT & Subramanian V (1984) In: Gibson DT (Ed), Microbial Degradation of Organic Hydrocarbons (pp 181–252). Marcel Dekker, New York, New York.

Gieg LM, Kolhatkar RV, McInerney M J, Tanner RS, Harris SH Jr, Sublette KL & Suflita JM (1999) Intrinsic bioremediation of petroleum hydrocarbons in a gas condensate-contaminated aquifer. Environ. Sci. Technol. 33: 2550–2560

Hohener P, Hunkeler D, Hess A, Bregnard T & Zeyer J (1998) Methodology for the evaluation of engineered in situ bioremediation: lessons from a case study. J. Microbiol. Meth. 32: 179–192

Holliger C & Zehnder AJB (1996) Anaerobic biodegradation of hydrocarbons. Cur. Opin. Biotechnol. 7: 326–330

Holman HY & Tsang YW (1995) Influence of soil moisture on biodegradation of petroleum hydrocarbons. In: Hinchee RE, Miller RN & Johnson PC (Eds) In Situ Aeration: Air Sparging, Bioventing, and related remediation processes (pp 323–332). Battelle Press, Colombus, Ohio.

Hunkeler D, Hohener P, Bernasconi S & Zeyer J (1999) Engineered in situ bioremediation of a petroleum hydrocarbon-contaminated aquifer: assessment of mineralization based on alkalinity, inorganic carbon and stable carbon isotope balances. J. Contam. Hydrol. 37: 201–223

Kampbell DH, Wiedemeier TH & Hansen JE (1996) Intrinsic bioremediation of fuel contamination in ground water at a field site. J. Hazard. Mater. 49: 197–204

Krumholz L, Caldwell ME & Suflita JM (1996) Biodegradation of 'BTEX' hydrocarbons under anaerobic conditions. In: Crawford RL & Crawford DL (Eds), Bioremediation: Principles and Applications (pp 61–99). Cambridge University Press, Cambridge, Massachusetts

Madsen EL (1991) Determining in situ biodegradation: facts and challenges. Environ. Sci. Technol. 25: 1663–1673

McAllister PM & Chiang CY (1994) A practical approach to evaluating natural attenuation of contaminants in ground water. Ground Water Monitoring and Remediation 14: 161–173

PRC Environmental Management & Montgomery Watson (1993) Data Summary Report, Remedial Investigation/Feasibility Study Phases 1 & 2A. Naval Air Station, Alameda, California

PRC Environmental Management (1994) SCAPS Push and Intercalibration/Validation Boring Summary Report. Naval Air Station, Alameda, California

Rice DW, Dooher BP, Cullen SJ, Everett LG, Kastenberg WE, Grose RD & Marino MA (1995) Recommendation to Improve the Cleanup Process for California's Leaking Underground Fuel Tanks (LUFTs). Lawrence Livermore National Laboratory, Livermore, CA (UCRL-AR-12176)

Rifai HS, Borden RC, Wilson JT & Ward CH (1995) Intrinsic bioattenuation for subsurface restoration. In: Hinchee RE & Wilson JT & Downey DC (Eds) Intrinsic Bioremediation (pp 1–29). Battelle Press, Columbus, Ohio

Sinclair JL & Ghiorse WC (1989) Distribution of aerobic bacteria, protozoa, algae, and fungi in deep subsurface sediments. Geomicrobiol. J. 7: 15–31

So CM & Young LY (1999) Isolation and characterization of a sulfate-reducing bacterium that anaerobically degrades alkanes. Appl. Environ. Microbiol. 65(7): 2969–2976

U.S. National Research Council (1993) In Situ Bioremediation – When Does It Work? National Academy Press, Washington DC

U.S. National Research Council (1994) Alternatives for Ground Water Cleanup. National Academy Press, Washington DC

Wiedemeier TH, Swanson MA, Wilson JT, Kampbell DH, Miller RN & Hansen JE (1995) Patterns of intrinsic bioremediation at two U.S. Air Force Bases. In: Hinchee RE & Wilson JT & Downey DC (Eds) Intrinsic Bioremediation (pp 31–51). Battelle Press, Columbus, Ohio

Wiedemeier TH, Wilson JT, Kampbell DH, Miller RN & Hansen JE (1995) Technical Protocol for Implementing Intrinsic Remediation with Long-Term Monitoring for Natural Attenuation of Fuel Contamination Dissolved in Groundwater. Air Force Center for Environmental Excellence, Brooks Air Force Base, TX

Zengler K, Richnow HH, Rossello-Mora R, Michaelis W & Widdel F (1999) Methane formation from long-chain alkanes by anaerobic microorganisms. Nature 401(6750): 266–269